Prescribed Performance Motion Control: A Control Barrier Function Approach

Xinming Wang, *Graduate Student Member*, Yuan Jiang, Jun Yang, *IEEE Fellow*, Yunda Yan, *IEEE Member*, and Shihua Li, *IEEE Fellow*

***Abstract*—Prescribed performance control (PPC) has been widely applied in motion control systems due to its ability to regulate both transient and steady-state performance through well-defined performance functions. However, its core design ideas, involving error state transformation or reciprocal nonlinear gain, can lead to invalid results under certain initial conditions, significantly restricting its practical application. To address these issues, a new motion control approach with prescribed performance is investigated using the control barrier function (CBF) technique. The tracking control problem is formulated as a quadratic programming by modifying a baseline controller subject to the proposed prescribed performance CBF (PP-CBF) constraints, where the disturbance observer technique is employed to handle lumped disturbances, such as unknown friction and load torque. Unlike conventional PPC methods, this framework allows for initial states outside the performance envelope and mitigates potential singularity issues near the boundary. The stability of the optimization-based control policy is rigorously analyzed. Comparative experimental tests conducted on a permanent magnet synchronous motor (PMSM) platform illustrate the effectiveness of the proposed method in achieving the prescribed performance specifications and its adaptability to nonlocal initial conditions and suddenly added loads.**

***Index Terms*—Control barrier function, disturbance rejection, motion control, prescribed performance.**

I. Introduction

HIGH-performance motion control system has been a critical element in ensuring the efficiency, safety, and quality of a wide range of practical systems and applications, e.g., the robotics [1], [2], the unmanned aerial vehicles [3], [4], and the electrical vehicles [5], [6]. Over the past few decades, significant efforts have been devoted to developing advanced control methodologies that enhance the precision and robustness of control systems against uncertainties, external disturbances, and unmodeled dynamics [7]–[13]. However, providing explicit performance guarantees in both the transient and steady-state phases remains a challenge, but is increasingly demanded by emerging robotic and autonomous systems, such as ensuring the safe operation of manipulators [14], achieving smooth acceleration in autonomous vehicles [15] and executing aerial manipulation tasks with drones [16]. Meeting these requirements demands the continued research and development of controller design with explicit control performance.

To achieve the desired explicit tracking performance, two approaches have been proposed: funnel control (FC) [17], [18] and prescribed performance control (PPC) [19], [20]. These two control methods share the common characteristic of using a monotonically decreasing performance function to identify desired performance specifications such as maximum overshoot, minimum convergence rate, and maximum steady-state tracking error. While funnel control adjusts the control gain using a time-varying function that increases when the output tracking error approaches the predefined funnel boundary, PPC employs a state transformation technique to convert constrained control problems into the boundedness of a transformed variable. The PPC and FC control methodologies have been applied to different practical motion control systems [21]–[24]. To be specific, by constructing a friction compensation neural network, an adaptive control with prescribed performance constraint is proposed for a class of nonlinear mechanisms and tested on a two-axis turntable servo system in [21]. In [22], a backstepping-based funnel control approach is investigated for the position control of permanent magnet synchronous motors (PMSMs), where the extended state observer (ESO) is used to estimate the lumped disturbances. Integrating with the terminal sliding mode control, the prescribed performance speed control is developed for the linear traction system by utilizing the disturbance observer [23]. To improve the tracking performance in steady-state phase, based on the dynamic surface control technique, a practical finite-time funnel control is studied and verified on a two-joint robot arm [24].

These noteworthy works guarantee the prescribed performance tracking tasks for different systems, but they impose a strict condition on the initial state, which will complicate real-world implementation. Additionally, the closed-loop system may become unstable if the states deviate from the interior of the performance envelope with suddenly added disturbances or measurement errors. To address these issues, theoretical advances have been proposed. In [25], an interval theory-based switching controller is suggested for a class of nonlinear systems, addressing the issue of infinite control energy. Additionally, [26] introduces a novel prescribed performance

Xinming Wang, Yuan Jiang and Shihua Li are with the Key Laboratory of Measurement and Control of CSE, Ministry of Education, School of Automation, Southeast University, Nanjing 210096, China. (email: wxm_seu@seu.edu.cn, yuan_jiang@seu.edu.cn, lsh@seu.edu.cn).

Jun Yang is with Department of Aeronautical and Automotive Engineering, Loughborough University, Loughborough LE11 3TU, UK (e-mail: j.yang3@lboro.ac.uk).

Yunda Yan is with Department of Computer Science, University College London, London, WC1E 6BT, UK (e-mail: yunda.yan@ucl.ac.uk).

controller with a flexible performance function mechanism for nonlinear systems subject to input saturation, where the performance function increases when input saturation occurs. This concept is further explored in [27] for a class of nonlinear systems within the FC framework. However, these innovative approaches require a redesign of the controller, increasing the complexity of implementation.

Recently, the control barrier function (CBF)-based control approach has emerged as an effective tool to achieve formal safety constraints for safety-critical systems by guaranteeing the forward invariance of a specified safety set [28]–[30]. In the context of CBF-based control, the desired forward invariant performance can be achieved by modifying conventional controller with the CBF constraints. Moreover, the CBF can drive the system asymptotically to the boundary of the safety set if the initial states are outside that set. These potentials offer the possibility of developing a new approach to address the prescribed performance control task. Nevertheless, there are few works that address the prescribed performance control for CBF-based motion control systems with rigorous theoretical stability analysis. Moreover, conventional CBF-based approaches are also prone to be affected by external disturbances and unknown dynamics, increasing the difficulty in controller design and analysis.

In this paper, leveraging the benefits of CBF, we introduce a new prescribed performance motion control (PPMC) approach for a class of motion control systems with disturbances. To address the limitations in conventional PPC methods, explicit performance constraints are interpreted as two compatible prescribed performance CBF (PP-CBF) constraints on the control input, where the disturbance estimation and compensation technique [31] is employed to enhance robustness. Based on the proposed PP-CBFs, an optimization-based control policy is constructed by modifying the baseline controller to guarantee the prescribed performance constraint and the precise tracking performance, simultaneously. Incorporating the sharing CBFs and piecewise quadratic Lyapunov function techniques [32], [33], the global stability of the closed-loop system is established under certain mild conditions. To validate the effectiveness of the proposed approach, experimental tests are conducted on a permanent magnet synchronous motor (PMSM) test platform under different initial states and load conditions. The results showcase the effectiveness of the proposed method in achieving the prescribed performance objective and its versatility in handling nonlocal initial conditions and sudden load changes. The main contributions are concluded as follows

1) Different from the conventional FC or PPC methodology, an alternative prescribed performance control framework is developed based on the CBF for a class of motion control systems, which eliminates the strict initial condition constraints and addresses potential singularity issues.
2) Incorporating with the sharing CBFs and piecewise quadratic Lyapunov function techniques [32], [33], sufficient conditions guaranteeing the global stability are theoretically derived.
3) Comparative experimental tests are conducted on a PMSM platform with different initial state and load conditions, demonstrating the effectiveness of the proposed control approach and its adaptability in practical use.

Notation: Sets of real numbers and nonnegative integers are denoted as $\mathbb{R}$ and $\mathbb{N}$. For $i, j \in \mathbb{N}$ satisfying $i \leq j$, define $\mathbb{N}_{i:j} \triangleq \{i, i+1, \cdots, j\}$ as a subset of $\mathbb{N}$. The identity matrix is denoted as $\boldsymbol{I}_n$ with size n. Denote $\lambda_{\max}(\boldsymbol{P})$ as the maximum eigenvalue of a given matrix $\boldsymbol{P}$. Define $\boldsymbol{O}_{m\times n}$ as a zero matrix of order $m \times n$. Denote $\boldsymbol{M} \succ 0$, $\boldsymbol{M} \succeq 0$, $\boldsymbol{M} \prec 0$ and $\boldsymbol{M} \preceq 0$ for positive-definite, positive semi-definite, negative-definite and negative semi-definite matrices, respectively. A continuous function $\alpha_e : (-b, a) \to (-\infty, \infty)$ is said to belong to the extended class $\mathcal{K}$ function for some $a, b > 0$ if it is strictly increasing and $\alpha_e(0) = 0$. Define $\|\boldsymbol{x}\|$ as the 2-norm of vector $\boldsymbol{x}$.

II. Preliminaries and problem formulation

In this section, the basic notion of a control barrier function is first introduced. Then, the mathematical model of the studied motion control system is presented along with the description of the prescribed performance tracking task.

A. Control barrier function

Consider the following nonlinear system

$$\dot{\boldsymbol{x}} = \boldsymbol{f}(\boldsymbol{x}) + \boldsymbol{g}(\boldsymbol{x})\boldsymbol{u}, \tag{1}$$

where $\boldsymbol{x} \in \mathbb{X} \subseteq \mathbb{R}^n$, $\boldsymbol{u} \in \mathbb{R}^m$ are the states and the control inputs, $\mathbb{X}$ is the admissible set of state. Nonlinear functions $\boldsymbol{f} : \mathbb{R}^n \to \mathbb{R}^n$, $\boldsymbol{g} : \mathbb{R}^n \to \mathbb{R}^{n\times m}$ are Lipschitz continuous functions. Taking into account a continuously differentiable function $h : \mathbb{R}^n \to \mathbb{R}$, we define the following 0-superlevel set

$$C = \{\boldsymbol{x} \in \mathbb{R}^n | h(\boldsymbol{x}) \geq 0\}. \tag{2}$$

Denote $\partial C := \{\boldsymbol{x} \in \mathbb{R}^n | h(\boldsymbol{x}) = 0\}$ and $\mathrm{Int}(C) := \{\boldsymbol{x} \in \mathbb{R}^n | h(\boldsymbol{x}) > 0\}$ as the boundary and interior of the set C. In the framework of CBF, if there exists a control input $\boldsymbol{u}$ makes the set C a forward invariant set, i.e., the trajectory $\boldsymbol{x}(t) \in C$, $\forall t > 0$, if $\boldsymbol{x}(0) \in C$, then the system is able to guarantee the constraints specified by C.

Definition 1. *[29] Considering the nonlinear system (1), the continuously differentiable function $h(\boldsymbol{x})$ is a CBF, if there exists an extended class $\mathcal{K}$ function $\alpha_e(\cdot)$ subject to*

$$\sup_{u\in\mathbb{R}^m} \{L_{\boldsymbol{f}} h(\boldsymbol{x}) + L_{\boldsymbol{g}} h(\boldsymbol{x})\boldsymbol{u} + \alpha_e(h(\boldsymbol{x}))\} \geq 0, \ \forall \boldsymbol{x} \in \mathbb{X}, \tag{3}$$

where $L_{\boldsymbol{f}} h(\boldsymbol{x}) = \frac{\partial h(\boldsymbol{x})}{\partial \boldsymbol{x}} \boldsymbol{f}(\boldsymbol{x})$ and $L_{\boldsymbol{g}} h(\boldsymbol{x}) = \frac{\partial h(\boldsymbol{x})}{\partial \boldsymbol{x}} \boldsymbol{g}(\boldsymbol{x})$ are standard Lie derivatives.

If there exists a CBF $h(\boldsymbol{x})$, then any Lipschitz continuous control action $\boldsymbol{u}(t) \in K_{CBF} := \{u \in \mathbb{R}^m | L_{\boldsymbol{f}} h(\boldsymbol{x}) + L_{\boldsymbol{g}} h(\boldsymbol{x})u + \alpha_e(h(\boldsymbol{x})) \geq 0\}$ renders the set C forward invariant.

B. Problem formulation

In this paper, we consider the following nonlinear motion control system

$$\begin{aligned} \dot{\xi}_1 &= \xi_2, \\ \dot{\xi}_2 &= g(\xi_1, \xi_2) + bu + d, \end{aligned} \tag{4}$$

where ξ_1, ξ_2 are the position and velocity of the motion control system, $g(\xi_1, \xi_2)$ is the known nonlinear function, b is the known control gain, u is the control input and d is the lumped disturbance containing external load and unknown dynamics. Without the loss of generality, the control gain b is considered as a positive value. It should be highlighted that the considered system (4) includes many practical systems like PMSM [22], linear traction system [23] and one joint rotary system [34].

Define the tracking error $e(t) = \xi_1(t) - \xi_d(t)$, where $\xi_d(t)$ is the desired reference signal. Then, it is obtained that

$$\begin{aligned} \dot{x}_1 &= x_2, \\ \dot{x}_2 &= f(\xi_1, \xi_2, \ddot{\xi}_d) + bu + d, \end{aligned} \tag{5}$$

where $x_1 = e$, $x_2 = \xi_2 - \dot{\xi}_d$, $f(\xi_1, \xi_2, \ddot{\xi}_d) = g(\xi_1, \xi_2) - \ddot{\xi}_d$. The control objective of this study is to design a proper $u(t)$ to make the tracking error $e(t)$ converge to zero and satisfy the prescribed performance constraint expressed as follows

$$-p_1(t) \leq x_1(t) \leq p_2(t), \forall t > 0, \tag{6}$$

where $p_1(t)$ and $p_2(t)$ are pre-defined smooth performance functions to specify the desired transient and steady-state performances, e.g., the maximum overshoot, the minimum settling time and the maximum steady-state tracking error. In this paper, the exponentially decreasing type performance functions are considered, which can be uniformly presented as follows

$$p_i(t) = p_{i,0} e^{-a_i t} + p_{i,\infty},\ i \in \mathbb{N}_{1:2}, \tag{7}$$

where $p_{i,0} > p_{i,\infty} > 0$ are constants interpreting the performance boundary, and $a_i > 0$ are used to regulate the decaying rate of performance functions.

Assumption 1. *The desired position signal $\xi_d(t)$ and its derivatives $\dot{\xi}_d(t)$ and $\ddot{\xi}_d(t)$ are assumed to be known smooth signals. Meanwhile, in this study, the disturbance d is assumed as an unknown time-varying signal satisfying $|d| \leq \delta_0$ and $|\dot{d}| \leq \delta_1$, where δ_0 and δ_1 are known positive constants.*

III. Prescribed performance motion control design

In this section, the prescribed performance motion control policy is adopted by proposing a new CBF encoding the desired performance specification. Before introducing the proposed approach, the design of disturbance observer is first presented.

A. Disturbance observer design and estimation error quantification

Considering the dynamics of error system (5), the disturbance observer employed from [35] is constructed as follows

$$\begin{aligned} \dot{z} &= -L(f + bu + z + Lx_2), \\ \hat{d} &= z + Lx_2, \end{aligned} \tag{8}$$

where z is the auxiliary state, $L > 0$ is the observer parameter to be designed and $\hat{d}$ is the estimate of d. Defining estimation error $e_d = d - \hat{d}$, then it is obtained that

$$\dot{e}_d = -Le_d + \dot{d}. \tag{9}$$

From the dynamics of (9) and Assumption 1, e_d is input-to-state stable [36] with respect to $\dot{d}(t)$. By selecting the zero initial value of $\hat{d}(0)$, the solution of above error dynamics can be over-estimated as

$$\begin{aligned} |e_d(t)| &= |e^{-Lt} e_d(0) + \int_0^t e^{-L(t-\tau)} \dot{d}(\tau) \mathrm{d}\tau| \\ &\leq \delta_0 e^{-Lt} + \delta_1 \int_0^t |e^{-L(t-\tau)}| \mathrm{d}\tau. \end{aligned} \tag{10}$$

By solving the above integral, the following estimation error bound is obtained

$$\epsilon(t) = \left(\delta_0 - \frac{1}{L}\delta_1\right) e^{-Lt} + \frac{1}{L}\delta_1. \tag{11}$$

In the next section, the $\hat{d}$ will be used to compensate for the real disturbance in the dynamics of CBF and the estimation error bound $\epsilon(t)$ will be utilized to dominate the impacts caused by the estimation error.

B. Prescribed performance CBF design

To achieve the desired tracking constraint in (6), the following two continuously differentiable functions are utilized to interpret the prescribed performance specification

$$\begin{aligned} h_1(t, x_1) &= x_1(t) + p_1(t), \\ h_2(t, x_1) &= p_2(t) - x_1(t). \end{aligned} \tag{12}$$

Inspired by the virtue of CBFs, if there exists a control $u(t)$ such that all $h_1(t, x_1)$ and $h_2(t, x_1)$ are positive, then the prescribed performance is achieved. Toward this end, we define the following auxiliary states

$$\begin{aligned} \phi_1 &= \dot{h}_1 + l_1 h_1, \\ \phi_2 &= \ddot{h}_1 + (l_1 + l_2)\dot{h}_1 + l_1 l_2 h_1, \\ \psi_1 &= \dot{h}_2 + l_1 h_2, \\ \psi_2 &= \ddot{h}_2 + (l_1 + l_2)\dot{h}_2 + l_1 l_2 h_2, \end{aligned} \tag{13}$$

where l_1, l_2 are positive constants to be designed. We further define the following 0-superlevel sets as

$$\begin{aligned} C_{1,0} &= \{[x_1, x_2]^T \in \mathbb{R}^2 | h_1(t, x_1) \geq 0\}, \\ C_{2,0} &= \{[x_1, x_2]^T \in \mathbb{R}^2 | h_2(t, x_1) \geq 0\}, \\ C_{1,1} &= \{[x_1, x_2]^T \in \mathbb{R}^2 | \phi_1(t, x_1, x_2) \geq 0\}, \\ C_{2,1} &= \{[x_1, x_2]^T \in \mathbb{R}^2 | \psi_1(t, x_1, x_2) \geq 0\}. \end{aligned} \tag{14}$$

Then, we can present the proposed PP-CBFs design.

Definition 2. *(PP-CBFs) Consider the system (5) and the disturbance observer (8) with Assumption 1. The time-varying functions $h_1(t, x_1)$ and $h_2(t, x_1)$ are the PP-CBFs, if there exist positive parameters l_1 and l_2 such that the following set of control input is not empty*

$$K_{PP-CBF} := \{u \in \mathbb{R} | \alpha_1 + \beta_1 u \geq 0 \text{ and } \alpha_2 + \beta_2 u \geq 0\}, \tag{15}$$

for all $\boldsymbol{x} := [x_1, x_2]^T \in \bar{C}$ and $\bar{C} := C_{1,0} \cap C_{1,1} \cap C_{2,0} \cap C_{2,1}$, where

$$\begin{aligned} \alpha_1 &= f + (l_1 + l_2)\dot{h}_1 + l_1 l_2 h_1 + \ddot{p}_1 + \hat{d} - \epsilon,\ \beta_1 = b \\ \alpha_2 &= -f + (l_1 + l_2)\dot{h}_2 + l_1 l_2 h_2 + \ddot{p}_2 - \hat{d} - \epsilon,\ \beta_2 = -b. \end{aligned} \tag{16}$$

The following theorem provides the sufficient conditions that there exists a Lipschitz continuous controller from K_{PP-CBF} that renders the $\bar{C}$ forward invariant, i.e., the prescribed performance constraints can be achieved.

Theorem 1. *Consider the system (5) and a well-designed disturbance observer (8) with Assumption 1. If the initial conditions of $h_1(0, x_1(0))$, $h_2(0, x_1(0))$, $\phi_1(0, x_1(0), x_2(0))$ and $\psi_1(0, x_1(0), x_2(0))$ are positive, and the following conditions further hold,*

$$l_1 l_2 p_i(t) + (l_1 + l_2)\dot{p}_i(t) + \ddot{p}_i(t) \geq \epsilon(t),\ i \in \mathbb{N}_{1:2}, \tag{17}$$

then any Lipschitz continuous controllers belong to (15) renders the set $\bar{C}$ forward invariant for the tracking error system (5).

Proof. As shown in (15), the prescribed performance constraints can be expressed as the following two inequalities on control input

$$\begin{aligned} bu &\geq -f - (l_1 + l_2)\dot{h}_1 - l_1 l_2 h_1 - \ddot{p}_1 - \hat{d} + \epsilon, \\ bu &\leq -f + (l_1 + l_2)\dot{h}_2 + l_1 l_2 h_2 + \ddot{p}_2 - \hat{d} - \epsilon. \end{aligned} \tag{18}$$

It can be obtained that if (17) is satisfied, the set K_{PP-CBF} is not empty. Then, substituting (18) into the dynamics of ϕ_2 and ψ_2, we have

$$\begin{aligned} \phi_2 &\geq d - \hat{d} + \epsilon, \\ \psi_2 &\geq \hat{d} - d + \epsilon. \end{aligned} \tag{19}$$

Due to the fact that $\epsilon(t) \geq |e_d(t)|$ from (11), it is obtained that $\phi_2(t) \geq 0$ and $\psi_2(t) \geq 0, \forall t > 0$. Rewriting the dynamics of (13), it is obtained that

$$\begin{aligned} \dot{h}_1 &= -l_1 h_1 + \phi_1,\ \dot{\phi}_1 = -l_2\phi_1 + \phi_2 \\ \dot{h}_2 &= -l_1 h_2 + \psi_1,\ \dot{\psi}_1 = -l_2\psi_1 + \psi_2 \end{aligned} \tag{20}$$

Since the initial values of ϕ_1 and ψ_1 are positive, it is obtained that ϕ_1 and ψ_1 are positive such that $C_{1,1}$ and $C_{2,1}$ are forward invariant from (13). Similarly, the sets $C_{1,0}$ and $C_{2,0}$ are also forward invariant with $h_1(0, x_1(0)) \geq 0$ and $h_2(0, x_1(0)) \geq 0$. Therefore, the forward invariant property of set $\bar{C}$ is guaranteed such that the prescribed performance constraints are satisfied. □

C. Prescribed performance CBF-based control design

Regarding the specification of the prescribed performance constraints by PP-CBFs, accurate position tracking is the other goal that needs to be achieved. To this end, the following PPMC quadratic programming (PPMC-QP)-based control policy is proposed by modifying a baseline tracking controller $v(t)$ with PP-CBFs

$$\begin{aligned} u^* = \arg\min_{u \in \mathbb{R}}\ & \frac{1}{2}(u - v)^2, && \textbf{PPMC QP} \\ \text{s.t.}\quad & \alpha_1 + \beta_1 u \geq 0, && \textbf{C1} \\ & \alpha_2 + \beta_2 u \geq 0. && \textbf{C2} \end{aligned} \tag{21}$$

The robust tracking controller v based on the notion of disturbance-observer-based control (DOBC) is designed as follows

$$v = -\frac{1}{b}[k_1 x_1 + k_2 x_2 + f(\xi_1, \xi_2, \ddot{\xi}_d) + \hat{d}], \tag{22}$$

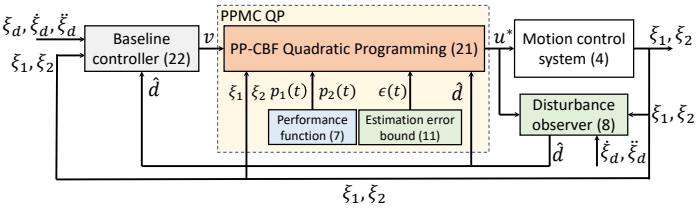

Fig. 1: The control block of the proposed motion control approaches.

where k_1, k_2 are the positive parameters to be designed. The schematic block of the proposed prescribed performance motion control approach is presented in Fig. 1. With the proposed control approach in (21), the prescribed performance tracking task can be achieved. Moreover, if the initial condition is located outside the performance boundary, the system will enter the performance envelope in finite time first and then converge to the reference. To rigorously demonstrate this, we present Theorem 2.

D. Stability analysis

To analyze the stability of the closed-loop system, we first solve the explicit form of (21) by using the Karush-Kuhn-Tucker (KKT) condition in [37]. Consider the following Lagrangian function,

$$\begin{aligned} \mathcal{L} =& \frac{1}{2}(u - v)^2 + \lambda_1[-bu - (l_1 + l_2)\dot{h}_1 - l_1 l_2 h_1 - \ddot{p}_1 - f \\ & - \hat{d} + \epsilon] + \lambda_2[bu - (l_1 + l_2)\dot{h}_2 - l_1 l_2 h_2 - \ddot{p}_2 + f + \hat{d} \\ & + \epsilon], \end{aligned} \tag{23}$$

where λ_1 and λ_2 are Lagrangian multipliers. Depending on whether the two performance constraints are active, the optimized controller can be solved as follows

$$u = \begin{cases} v, & \boldsymbol{x} \in \Omega_0 \\ -\frac{1}{b}[l_1 l_2 h_1 + (l_1 + l_2)\dot{h}_1 + \ddot{p}_1 + f + \hat{d} - \epsilon], & \boldsymbol{x} \in \Omega_1 \\ \frac{1}{b}[l_1 l_2 h_2 + (l_1 + l_2)\dot{h}_2 + \ddot{p}_2 - f - \hat{d} - \epsilon], & \boldsymbol{x} \in \Omega_2 \end{cases}, \tag{24}$$

with

$$\begin{aligned} \Omega_0 :=& \{\boldsymbol{x} \in \mathbb{R}^2 | \boldsymbol{E}_1^T \boldsymbol{x} + \sigma_1 \geq 0 \text{ and } \boldsymbol{E}_2^T \boldsymbol{x} + \sigma_2 \geq 0\}, \\ \Omega_1 :=& \{\boldsymbol{x} \in \mathbb{R}^2 | \boldsymbol{E}_1^T \boldsymbol{x} + \sigma_1 \leq 0 \text{ and } \boldsymbol{E}_2^T \boldsymbol{x} + \sigma_2 \geq 0\}, \\ \Omega_2 :=& \{\boldsymbol{x} \in \mathbb{R}^2 | \boldsymbol{E}_1^T \boldsymbol{x} + \sigma_1 \geq 0 \text{ and } \boldsymbol{E}_2^T \boldsymbol{x} + \sigma_2 \leq 0\}, \end{aligned} \tag{25}$$

where $\sigma_i = l_1 l_2 p_i + (l_1 + l_2)\dot{p}_i + \ddot{p}_i - \epsilon,\ i \in \mathbb{N}_{1:2}$, $\boldsymbol{E}_1 = [l_1 l_2 - k_1, l_1 + l_2 - k_2]^T$ and $\boldsymbol{E}_2 = [k_1 - l_1 l_2, k_2 - l_1 - l_2]^T$. Here, the parameters k_i and l_i satisfy $k_1 \neq l_1 l_2$ and $k_2 \neq l_1 + l_2$. The switching surfaces $\boldsymbol{E}_i^T \boldsymbol{x} + \sigma_i = 0$ are determined based on whether the constraints **C1** and **C2** in (21) are active, respectively. It should be highlighted that $\bigcup_{j=0}^{j=2} \Omega_j = \mathbb{R}^2$. Substituting (24) into (5), the closed-loop system can be rewritten as a piecewise linear systems

$$\dot{\boldsymbol{x}} = \begin{cases} \boldsymbol{A}\boldsymbol{x} + \boldsymbol{a}_0, & \boldsymbol{x} \in \Omega_0 \\ \boldsymbol{G}\boldsymbol{x} + \boldsymbol{a}_1, & \boldsymbol{x} \in \Omega_1 \\ \boldsymbol{G}\boldsymbol{x} + \boldsymbol{a}_2, & \boldsymbol{x} \in \Omega_2 \end{cases}, \tag{26}$$

with

$$\boldsymbol{A} = \begin{bmatrix} 0 & 1 \\ -k_1 & -k_2 \end{bmatrix}, \boldsymbol{G} = \begin{bmatrix} 0 & 1 \\ -l_1 l_2 & -l_1 - l_2 \end{bmatrix},$$

where $\boldsymbol{a}_0 = [0, e_d]^T$, $\boldsymbol{a}_1 = [0, -\sigma_1 + e_d]^T$, $\boldsymbol{a}_2 = [0, \sigma_2 + e_d]^T$. Augmenting the state $\boldsymbol{x}$ with σ_i in different partitions Ω_i, it is obtained that

$$\begin{aligned} \dot{\bar{\boldsymbol{x}}}_0 &= \bar{\boldsymbol{A}}\bar{\boldsymbol{x}}_0 + \boldsymbol{\delta}_0,\ \boldsymbol{x} \in \Omega_0 \\ \dot{\bar{\boldsymbol{x}}}_i &= \bar{\boldsymbol{G}}\bar{\boldsymbol{x}}_i + \boldsymbol{\delta}_i,\ \boldsymbol{x} \in \Omega_i \end{aligned} \tag{27}$$

where $\bar{\boldsymbol{x}}_0 = [x_1, x_2, 0]^T$, $\bar{\boldsymbol{x}}_1 = [x_1, x_2, -\sigma_1]^T$, $\bar{\boldsymbol{x}}_2 = [x_1, x_2, \sigma_2]^T$, $\boldsymbol{\delta}_0 = [0, e_d, 0]^T$, $\boldsymbol{\delta}_1 = [0, e_d, -\dot{\sigma}_1]^T$, $\boldsymbol{\delta}_2 = [0, e_d, \dot{\sigma}_2]^T$ and

$$\bar{\boldsymbol{A}} = \begin{bmatrix} 0 & 1 & 0 \\ -k_1 & -k_2 & 0 \\ 0 & 0 & 0 \end{bmatrix}, \bar{\boldsymbol{G}} = \begin{bmatrix} 0 & 1 & 0 \\ -l_1 l_2 & -l_1 - l_2 & 1 \\ 0 & 0 & 0 \end{bmatrix}.$$

Define

$$\boldsymbol{F}_0 = \begin{bmatrix} -\boldsymbol{k} & 0 \\ \boldsymbol{I}_2 & \boldsymbol{0}_{2\times 1} \end{bmatrix}, \boldsymbol{F}_i = \begin{bmatrix} -\boldsymbol{l} & 1 \\ \boldsymbol{I}_2 & \boldsymbol{0}_{2\times 1} \end{bmatrix}, \boldsymbol{k}^T = \begin{bmatrix} k_1 \\ k_2 \end{bmatrix},$$
$$\boldsymbol{l}^T = \begin{bmatrix} l_1 l_2 \\ l_2 + l_2 \end{bmatrix}, \bar{\boldsymbol{E}}_1 = \begin{bmatrix} -\boldsymbol{E}_1 & 1 \\ \boldsymbol{0}_{1\times 2} & -1 \end{bmatrix}, \bar{\boldsymbol{E}}_2 = \begin{bmatrix} -\boldsymbol{E}_2 & -1 \\ \boldsymbol{0}_{1\times 2} & 1 \end{bmatrix}.$$

Then, the stability of the closed-loop system is concluded in the following theorem.

Theorem 2. *Consider the system (5) and the disturbance observer (8) with Assumption 1. Given that the PP-CBFs $h_1(t, x_1)$ and $h_2(t, x_1)$ satisfy the following conditions*

$$k_1 p_i(t) + k_2 \dot{p}_i(t) + \ddot{p}_i(t) > (1 + m)\epsilon(t),\ i \in \mathbb{N}_{1:2}, \tag{28}$$

where $m \geq 4\lambda_{\max}(\boldsymbol{P}_G)\sqrt{(l_1 l_2 - k_1)^2 + (l_1 + l_2 - k_2)^2}$ and $\boldsymbol{P}_G$ is a symmetric positive definite matrix satisfying $\boldsymbol{G}^T\boldsymbol{P}_G + \boldsymbol{P}_G\boldsymbol{G} = -\boldsymbol{I}_2$. If there exist symmetric matrix $\boldsymbol{T}$ and positive definite matrices $\boldsymbol{M}_i$ and $\boldsymbol{N}_i$ satisfying

$$\boldsymbol{P}_0 \succ 0,\ \bar{\boldsymbol{A}}^T\boldsymbol{P}_0 + \boldsymbol{P}_0\bar{\boldsymbol{A}} \prec 0, \tag{29a}$$

$$\boldsymbol{P}_i \succ \bar{\boldsymbol{E}}_i^T\boldsymbol{N}_i\bar{\boldsymbol{E}}_i,\ \bar{\boldsymbol{G}}_i^T\boldsymbol{P}_i + \boldsymbol{P}_i\bar{\boldsymbol{G}}_i \prec -\bar{\boldsymbol{E}}_i^T\boldsymbol{M}_i\bar{\boldsymbol{E}}_i, \tag{29b}$$

and $\boldsymbol{P}_j = \boldsymbol{F}_j^T\boldsymbol{T}\boldsymbol{F}_j, j \in \mathbb{N}_{0:2}$, then the prescribed performance tracking task will be achieved and the tracking error will globally converge to a compact set around the origin.

For the sake of readability, the details of the stability analysis are given in the Appendix.

Remark 1. *Due to the space limit, only the case of $l_1 l_2 \neq k_1$ and $l_1 + l_2 \neq k_2$ is discussed, the other cases, e.g. $l_1 l_2 = k_1$ or $l_1 + l_2 = k_2$, can be analyzed following a similar way by constructing corresponding Lagrangian functions under certain conditions.*

Remark 2. *It should be highlighted that the proposed approach is capable of ensuring the strictly prescribed performance constraint with external torque that satisfies Assumption 1. In the presence of abnormal working conditions, such as sudden load changes, the tracking error may cross the performance boundary. The reason is that the error bound $\epsilon(t)$ in (11) decreases with time and cannot dominate the estimation error with a noncontinuous change. However, such an error will quickly decay and the position tracking error will renter the performance envelope following the results in Theorem 2.*

Remark 3. *In this paper, the disturbance observer from [35] is employed due to its ability to directly estimate the lumped disturbance and its ease of design. Generally, this observer can be substituted with other estimation techniques such as the extended state observer (ESO) [38], uncertainty disturbance estimator (UDE) [39], and equivalent-input-disturbance (EID) [40]. However, it is important to note that the corresponding estimation error quantization would require modification through the construction of a new Lyapunov function.*

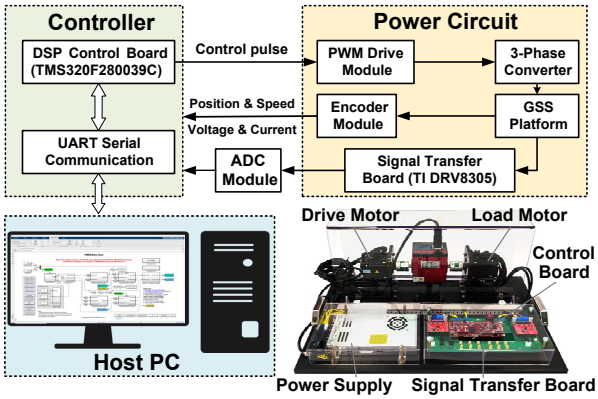

Fig. 2: Configuration of the experimental test platform.

Remark 4. *The control parameters for the baseline controller can be adjusted using classical disturbance observer-based control principles. Specifically, k_1 and k_2 can be chosen through methods such as pole placement or linear quadratic regulation, and L can be set to balance convergence rate and noise attenuation. Regarding the l_1 and l_2 derived from the PP-CBF, increasing l_1 expands the set $\bar{C}$ and thus eases the constraint on initial states according to Theorem 1. On the other hand, reducing l_2 prevents the tracking error from approaching the performance boundaries too closely. The estimation error bound ϵ has a direct impact on the active set of the baseline controller and can be adjusted following the condition (29).*

IV. Experimental Tests on PMSMs

In this section, to verify the effectiveness of the proposed approach, comparative experimental tests are conducted on a PMSM platform.

A. Mathematical model of PMSM

During the verification study in experiments, we only consider the control design of position and speed loops. The quick tracking dynamics of current loops (i.e., from current reference i_q^* to real current i_q) is ignored here by assuming that the current controllers are already well designed. Meanwhile, to obtain the maximum torque-to-current ratio, the reference value of the d-axis current i_d^* is set to zero. The PMSM system can be written as follows

$$\begin{aligned} \dot{\theta} &= w, \\ \dot{w} &= -\frac{B}{J}w + 1.5\frac{n_p\psi_f}{J}i_q - \frac{T_L}{J}, \end{aligned} \tag{30}$$

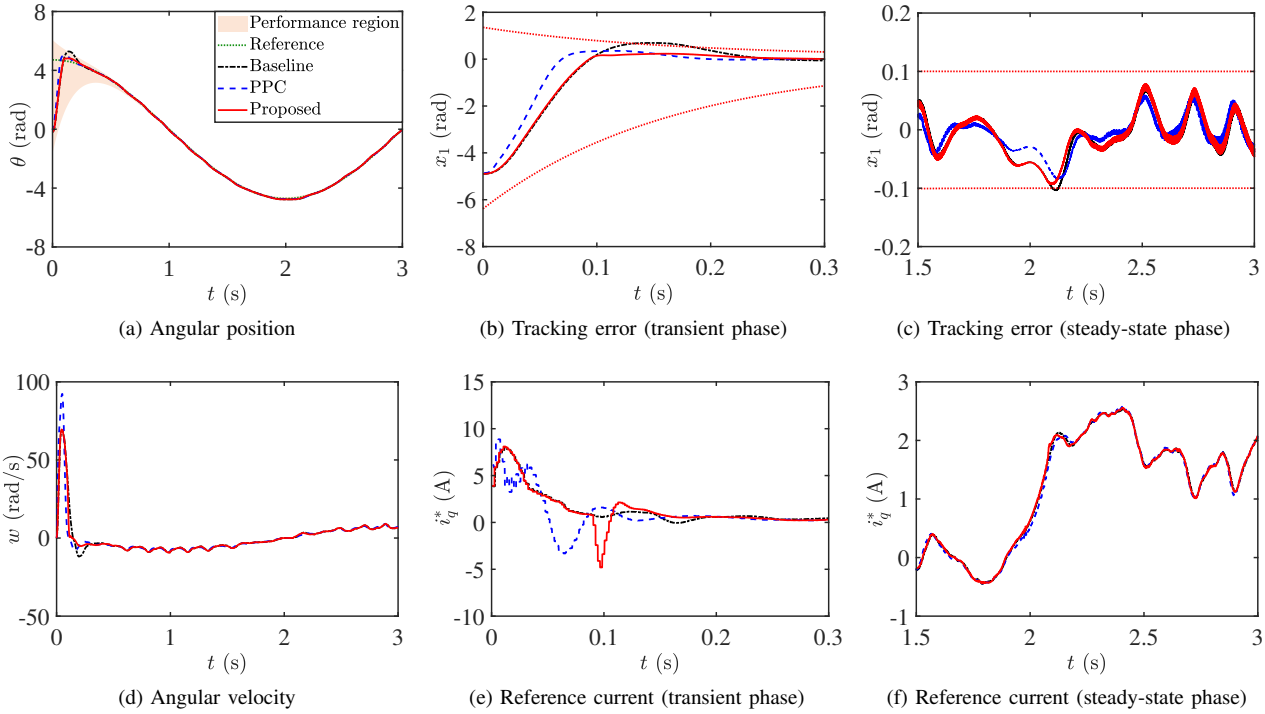

(a) Angular position (b) Tracking error (transient phase) (c) Tracking error (steady-state phase)

(d) Angular velocity (e) Reference current (transient phase) (f) Reference current (steady-state phase)

Fig. 3: Experimental results of Case I (prescribed performance tracking test). The performance functions are $p_1(t) = 2\pi e^{-6t} + 0.1$ rad and $p_2(t) = 0.4\pi e^{-6t} + 0.1$ rad, and load torque is $T_L = 0.1 + 0.05\sin(2\pi t)$ N $\cdot$ m.

where θ is the angular position, w is the angular velocity, n_p is the number of pole pairs, ψ_f is the rotor flux linkage, T_L is the load torque, J is the rotor inertia and B is the viscous frictional coefficient and i_q is the current of q-axis.

B. Experiment setup

The test platform, as shown in Fig. 2, is constructed based on the Texas Instruments C2000 development board (TSM320F280039C), and two low-voltage 3-phase sinusoidal permanent magnet motors (ASM200-36-2500) with embedded encoders, which are coupled in a dyno setup. One of the motors is controlled using the designed approach, while the other operates in torque control mode, serving as an external load. The switching frequency of the pulse width modulation (PWM) and the sampling frequency of the digital signal processor (DSP) are set at 20 kHz and 1 kHz, respectively. The electrical and mechanical parameters of the motors are $\psi_f = 1.2 \times 10^{-2}$ Wb, $J = 3.2 \times 10^{-5}$ kg $\cdot$ m^2, $B = 1.3 \times 10^{-3}$ N $\cdot$ m $\cdot$ s/rad and $n_p = 5$.

To fully examine the explicit desired tracking performance, the position reference is set as $\theta_d(t) = 1.5\pi\cos(\frac{\pi}{2}t)$rad in the following tests. Besides, the uncertainties consisting of both internal inertia perturbation (i.e., a variation of 10% percent below the nominal value) and external disturbance are imposed on the PMSM, which aims to investigate the robustness of the closed-loop system. Three cases are considered where the proposed controller is compared with the baseline as (22) and the traditional PPC developed in [21] as follows

$$u = \frac{1}{b}\Big\{-\frac{1}{r}[kS + \lambda\dot{\eta} + \dot{r}(x_2 - a_1x_1 + a_2x_1^2)] - f - \hat{d} + \dot{a}_1x_1 + a_1x_2 - \dot{a}_2x_1^2 - 2a_1x_1x_2\Big\}, \tag{31}$$

with

$$S = \dot{\eta} + k\eta,\ \eta = \ln\left(\frac{1+\frac{x_1}{p_1}}{1-\frac{x_1}{p_2}}\right),\ r = \frac{p_1+p_2}{(p_1+x_1)(p_2-x_1)},$$
$$a_1 = \frac{p_1^2\dot{p}_2 + p_2^2\dot{p}_1}{p_1p_2(p_1+p_2)},\ a_2 = \frac{p_2\dot{p}_1 - p_1\dot{p}_2}{p_1p_2(p_1+p_2)},$$

where η is the transformed state and k, λ are control parameters to be designed. The time-varying variables $\dot{r}$, $\dot{a}_1$ and $\dot{a}_2$ are relative derivatives. The performance functions are set as $p_1(t) = 2\pi e^{-6t}+0.1$ rad and $p_2(t) = 0.4\pi e^{-6t}+0.1$ rad. The saturation bound of the reference current i_q^* is set as 10 A. The control parameters of three control approaches are $k_1 = 1600$, $k_2 = 80$ for the baseline controller, $l_1 = 2000$, $l_2 = 50$ for PP-CBFs, $k = 65$, $\lambda = 65$ for the PPC controller, and $L = 1200$ for disturbance observer. These parameters are adjusted to achieve a comparable initial control effort and settling time.

C. Experiment results

1) Case I (prescribed performance tracking test): In this case, the prescribed performance tracking task is tested in the presence of load torque satisfying $T_L = 0.1+0.05\sin(2\pi t)$ N$\cdot$ m.

The experimental results are shown in Fig. 3 containing the curves of tracking error, angular velocity, and reference

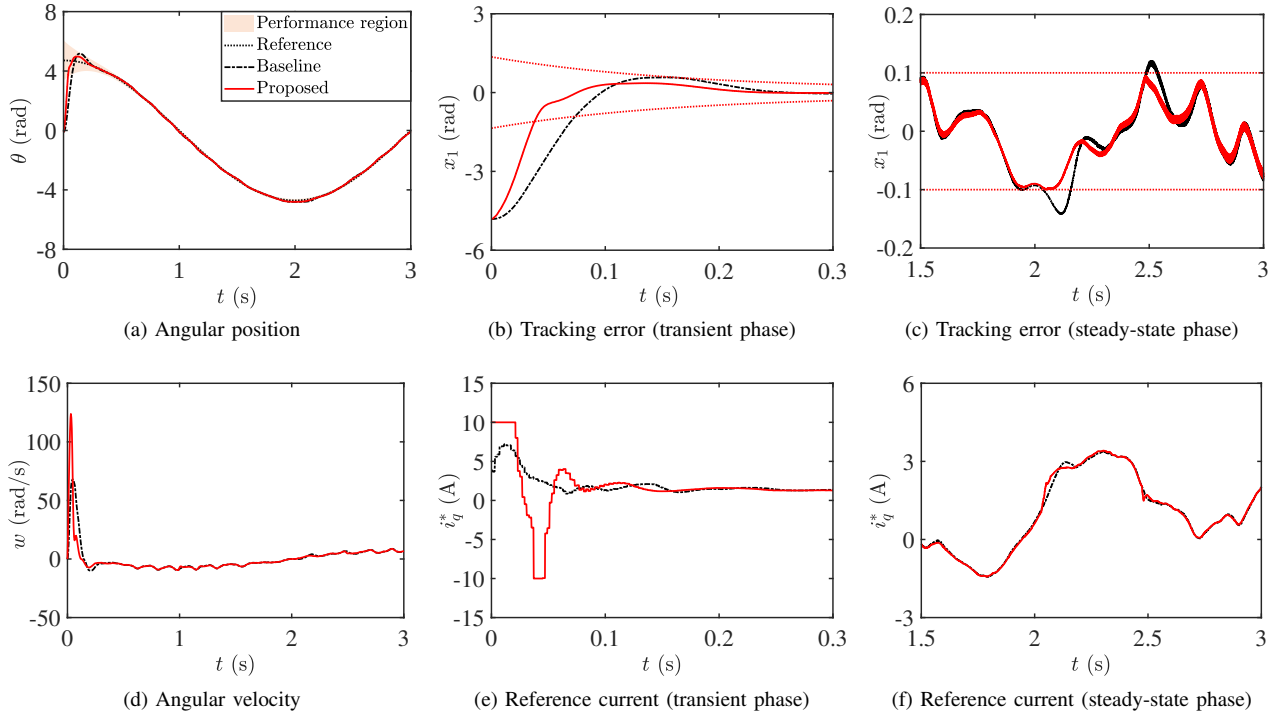

(a) Angular position (b) Tracking error (transient phase) (c) Tracking error (steady-state phase)

(d) Angular velocity (e) Reference current (transient phase) (f) Reference current (steady-state phase)

Fig. 4: Experimental results of Case II (nonlocal initial position error test). The performance functions are $p_1(t) = p_2(t) = 0.4\pi e^{-6t} + 0.1$ rad, and load torque is $T_L = 0.1 + 0.15\sin(2\pi t)$ N · m.

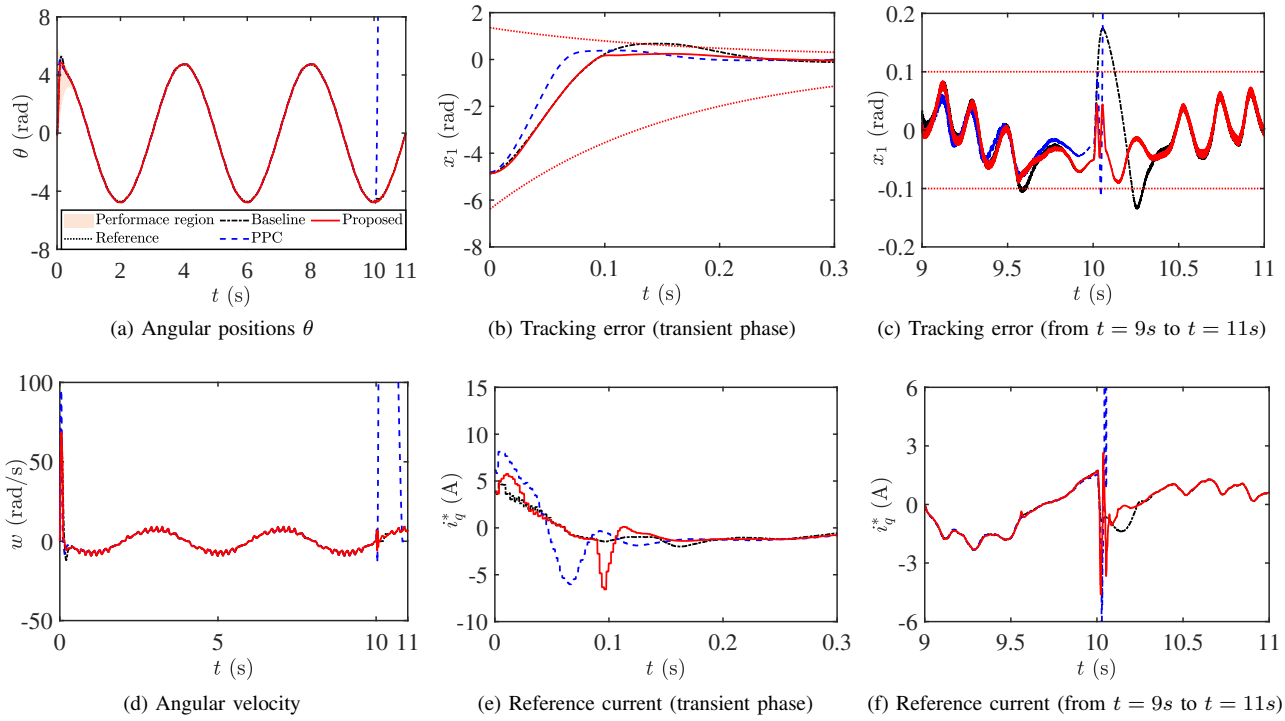

(a) Angular positions θ (b) Tracking error (transient phase) (c) Tracking error (from $t = 9s$ to $t = 11s$)

(d) Angular velocity (e) Reference current (transient phase) (f) Reference current (from $t = 9s$ to $t = 11s$)

Fig. 5: Experimental results of Case III (suddenly added disturbance test). The performance functions are same as Case I, and load torque is set as $T_L = 0.05 + 0.15\sin(\frac{3\pi}{2}t - \frac{\pi}{2})$ N · m, and it is changed to $T_L = -0.05 - 0.05\cos(\frac{3\pi}{2}t)$ N · m at $t = 10s$.

current. It is obtained that the proposed control scheme is able to achieve the desired tracking task with the prescribed performance constraint and presents similar accuracy as the traditional PPC scheme. Compared with the baseline approach, both the proposed approach and the PPC exhibit improved tracking error trajectories in both transient and steady-state phases, demonstrating their capability to regulate overshoots as they approach the performance boundary.

2) Case II (nonlocal initial position error test): To show the effectiveness of the proposed approach in relaxing the strictly

initial state condition, the performance functions are selected as $p_1(t) = p_2(t) = 0.4\pi e^{-6t} + 0.1$ rad, and a more intense load torque is set as $T_L = 0.1 + 0.15\sin(2\pi t)$ N$\cdot$m. Since the conventional PPC control does not work when $x(0) \leq -p_1(0)$ or $x(0) \geq p_2(0)$, we only compare the tracking performances of the proposed and baseline approaches in this case.

The experimental results including tracking error, velocity, and reference currents are shown in Fig. 4. When the initial error is outside the performance envelope, it is obtained that the proposed controller first drives the tracking error into the performance boundary, then it achieves the prescribed performance tracking task. Compared with the baseline controller, the proposed controller regulates the tracking performance in both the transient and steady-state phases.

3) Case III (suddenly added disturbance test): The presence of suddenly added load torque exists widely in PMSM-based applications. The following experiments are evaluated to show the control performances of the proposed method towards suddenly added disturbances. The load torque is set as $T_L = 0.05 + 0.15\sin(\frac{3\pi}{2}t - \frac{\pi}{2})$ N$\cdot$m, and it is changed to $T_L = -0.05 - 0.05\cos(\frac{3\pi}{2}t)$ N$\cdot$m at $t = 10s$.

The experimental results are shown in Fig. 5. In Fig. 5c, in the presence of suddenly added loads, the error of the baseline approach crosses the prescribed performance regions, while the proposed approach shows better control performance, since one of the constraints in PPMC-QP has become active. However, the closed-loop system under the PPC controller is not stable once the tracking error crosses the performance boundary, as the transferred state η becomes ill-defined in this situation.

V. Conclusion

In this paper, a new control methodology has been developed to achieve the prescribed performance motion control for a class of nonlinear motion systems. This new framework has provided an alternative but easier way to regulate the tracking performance with a relaxed condition on initial states and improved adaptability to suddenly added loads. To realize this goal, a quadratic programming problem has been constructed by modifying a baseline tracking controller with two compatible PP-CBFs designed to interpret the specified prescribed performances. The effectiveness of the proposed method has been verified through rigorous theoretical analysis and experimental tests of position control for PMSMs.

Appendix

A. Proof of Theorem 2

Proof. The proof is divided into two parts. We first show that if the initial conditions of $\boldsymbol{x}(0)$ are within the set $\bar{C}$, the prescribed performance constraints can be achieved and the tracking error converges to a compact set around the origin. Then, the stability of the closed-loop system is analyzed $\forall \boldsymbol{x}(0) \in \mathbb{R}^2/\bar{C}$. To briefly illustrate the dynamic behavior of the system, the state trajectories under the proposed controller (21) in the phase plane with constant performance functions $p_1(t), p_2(t)$ are shown in Fig. 6a. It should be highlighted that the depicted error state trajectories in Fig. 6 apply to the case

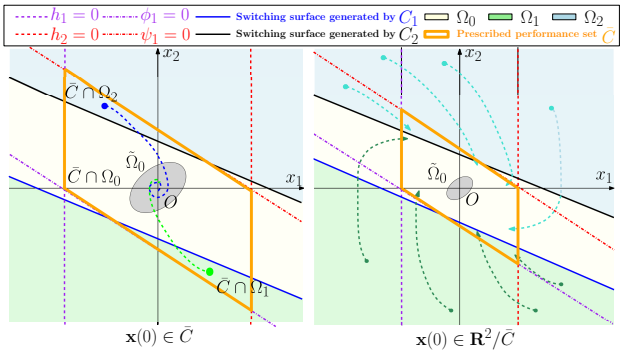

(a) State trajectories in phase plane

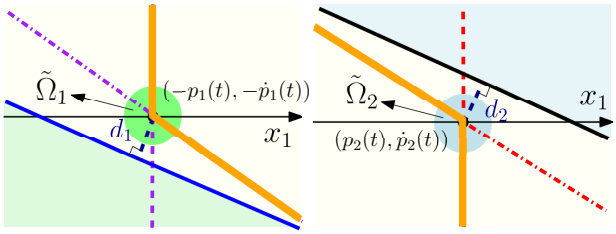

(b) Geometry relationships between $\tilde{\Omega}_1, \tilde{\Omega}_2$ and switching surfaces **C1**,**C2**

Fig. 6: Illustration of error states in phase plane with constant performance functions.

where $l_1 l_2 - k_1 > 0$ and $l_1 + l_2 - k_2 > 0$. Similar analyses can be conducted for other cases.

Part 1: From the results of Theorem 1, if $\boldsymbol{x}(0) \in \bar{C}$, it can be obtained that the prescribed performance constraints are achieved $\forall t \geq 0$.

As shown in (26), the closed-loop system has three potential attractors, i.e., $[-p_1(t), -\dot{p}_1(t)]^T$, $[p_2(t), \dot{p}_2(t)]^T$ and $[0, 0]^T$, in different partitions. In the following, we first show that there exists a compact set around the origin, which is the unique attraction region of the closed-loop system. This can be verified by comparing the distances from $[-p_1(t), -\dot{p}_1(t)]^T$ and $[p_2(t), \dot{p}_2(t)]^T$ to the switching surfaces $\boldsymbol{E}_i^T \boldsymbol{x} + \sigma_i = 0$, $i \in \mathbb{N}_{1:2}$ and the ultimate bound of $\|\boldsymbol{h}_i\|$. To this end, according to (26), the dynamics of $h_i(t, x)$ can be rewritten as

$$\dot{\boldsymbol{h}}_i = \boldsymbol{G}\boldsymbol{h}_i + \boldsymbol{\mu}_i, \ \boldsymbol{x} \in \Omega_i, \tag{32}$$

where $\boldsymbol{h}_i = [h_i, \dot{h}_i]^T$, $\boldsymbol{\mu}_1 = [0, \epsilon + d - \hat{d}]^T$ and $\boldsymbol{\mu}_2 = [0, \epsilon - d + \hat{d}]^T$. Selecting a candidate Lyapunov function as $V_h(\boldsymbol{h}_i) = \boldsymbol{h}_i^T \boldsymbol{P}_G \boldsymbol{h}_i$, its time derivative along the system (32) is

$$\begin{aligned} \dot{V}_h =& \boldsymbol{h}_i^T (\boldsymbol{G}^T \boldsymbol{P}_G + \boldsymbol{P}_G \boldsymbol{G}) \boldsymbol{h}_i + 2\boldsymbol{h}_i^T \boldsymbol{P}_G \boldsymbol{\mu}_i \\ \leq& - \|\boldsymbol{h}_i\|^2 + 4\epsilon \lambda_{\max}(\boldsymbol{P}_G) \|\boldsymbol{h}_i\|. \end{aligned} \tag{33}$$

Thus, the states $\boldsymbol{h}_i$ converge to the compact sets $\tilde{\Omega}_i := \{\boldsymbol{h} \in \mathbb{R}^2 | \|\boldsymbol{h}_i\| \leq 4\epsilon \lambda_{\max}(\boldsymbol{P}_G)\}$. According to [41], the distances d_i from $[-p_1(t), -\dot{p}_1(t)]^T$ and $[p_2(t), \dot{p}_2(t)]^T$ to the switching surfaces $\boldsymbol{E}_i^T \boldsymbol{x} + \sigma_i = 0$ are

$$d_i = \frac{k_1 p_i(t) + k_2 \dot{p}_i(t) + \ddot{p}_i(t) - \epsilon}{\sqrt{(l_1 l_2 - k_1)^2 + (l_1 + l_2 - k_2)^2}}. \tag{34}$$

Considering the conditions (28), it can be concluded that $\tilde{\Omega}_i$ is located in the set Ω_0. The geometry relationships between

the $\tilde{\Omega}_i$ and the switching surfaces are demonstrated in Fig. 6b. Meanwhile, considering a candidate Lyapunov function $V_a = \boldsymbol{x}^T \boldsymbol{P}_A \boldsymbol{x}$ with $\boldsymbol{A}^T \boldsymbol{P}_A + \boldsymbol{P}_A \boldsymbol{A} = -\boldsymbol{I}_2$, its derivative along the subsystem of (26) when $\boldsymbol{x} \in \Omega_0$ is

$$\dot{V}_a = \boldsymbol{x}^T (\boldsymbol{A}^T \boldsymbol{P}_A + \boldsymbol{P}_A \boldsymbol{A}) \boldsymbol{x} + 2\boldsymbol{x}^T \boldsymbol{P}_A \boldsymbol{a}_0. \tag{35}$$

Then, since $\boldsymbol{a}_0 = [0, e_d]^T$ is ultimately bounded, there exists a sublevel set $\tilde{\Omega}_0 = \{\boldsymbol{x} \in \mathbb{R}^2 | \boldsymbol{x}^T \boldsymbol{P}_A \boldsymbol{x} \leq l,\ l > 0\}$ such that once the states enter this set, they will not escape from it.

Next, to analyze the stability of the closed-loop system, the following piecewise quadratic Lyapunov functions are constructed

$$V(\bar{\boldsymbol{x}}) = \begin{cases} \bar{\boldsymbol{x}}_0^T \boldsymbol{P}_0 \bar{\boldsymbol{x}}_0, & \boldsymbol{x} \in \Omega_0 \\ \bar{\boldsymbol{x}}_i^T \boldsymbol{P}_i \bar{\boldsymbol{x}}_i, & \boldsymbol{x} \in \Omega_i, \end{cases} . \tag{36}$$

It can be verified that the selected Lyapunov function (36) is continuous on the switching surfaces $\boldsymbol{E}_i^T \boldsymbol{x} + \sigma_i = 0$, i.e., $\boldsymbol{F}_0 \bar{\boldsymbol{x}}_i = \boldsymbol{F}_i \bar{\boldsymbol{x}}_i$ when $\boldsymbol{E}_i^T \boldsymbol{x} + \sigma_i = 0$. Its time derivative along the augmented system (27) is

$$\dot{V}(\bar{\boldsymbol{x}}) = \begin{cases} \bar{\boldsymbol{x}}_0^T (\bar{\boldsymbol{A}}^T \boldsymbol{P}_0 + \boldsymbol{P}_0 \bar{\boldsymbol{A}}) \bar{\boldsymbol{x}}_0 + 2\bar{\boldsymbol{x}}_0^T \boldsymbol{P}_0 \boldsymbol{\delta}_0,\ \boldsymbol{x} \in \Omega_0, \\ \bar{\boldsymbol{x}}_i^T (\bar{\boldsymbol{G}}^T \boldsymbol{P}_i + \boldsymbol{P}_i \bar{\boldsymbol{G}}) \bar{\boldsymbol{x}}_i + 2\bar{\boldsymbol{x}}_i^T \boldsymbol{P}_i \boldsymbol{\delta}_i,\ \boldsymbol{x} \in \Omega_i \end{cases} . \tag{37}$$

The perturbation terms $\boldsymbol{\delta}_j,\ j \in \mathbb{N}_{0:2}$ in (37) are ultimately bounded, whose amplitude is determined by the estimation error e_d and the exponentially decaying functions $\dot{\sigma}_i$. Since the condition (29) is satisfied, there exist positive constants $\eta_j,\ j \in \mathbb{N}_{0:2}$, such that

$$\dot{V}(\bar{\boldsymbol{x}}) \leq -\eta_i \|\bar{\boldsymbol{x}}_i\|^2 + 2\bar{\boldsymbol{x}}_i^T \boldsymbol{P}_i \boldsymbol{\delta}_i,\ \forall \boldsymbol{x} \in \Omega_i, \tag{38}$$

Similar to analysis in (33), it is obtained that $\dot{V}(\bar{\boldsymbol{x}}) \leq 0,\ \forall \bar{\boldsymbol{x}} \in \Omega_i \times \mathbb{R} / \Upsilon_i$, where $\Upsilon_i := \{\bar{\boldsymbol{x}} \in \mathbb{R}^3 | \|\bar{\boldsymbol{x}}\| \leq \frac{2\lambda_{\max}(\boldsymbol{P}_i)}{\eta_i} \|\boldsymbol{\delta}_i\|\}$. It should be noted that these sets can be adjusted as small as possible by properly increasing the observer gain L such that sets Υ_i are the subsets of $\Omega_0 \times \mathbb{R}$. If $\boldsymbol{x} \in \Omega_0$, it is obtained that

$$\dot{V}(\bar{\boldsymbol{x}}) \leq -\eta_0 \|\bar{\boldsymbol{x}}_0\|^2 + 2\bar{\boldsymbol{x}}_0^T \boldsymbol{P}_0 \boldsymbol{\delta}_0,\ \forall \boldsymbol{x} \in \Omega_0, \tag{39}$$

Then, we have $\dot{V}(\bar{\boldsymbol{x}}) \leq 0,\ \forall \bar{\boldsymbol{x}} \in \Omega_0 \times \mathbb{R} / \Upsilon_0$, where $\Upsilon_0 := \{\bar{\boldsymbol{x}} \in \mathbb{R}^3 | \|\bar{\boldsymbol{x}}\| \leq \frac{2\lambda_{\max}(\boldsymbol{P}_0)}{\eta_0} \|\boldsymbol{\delta}_0\|\}$.

Thus, it can be concluded that $\dot{V}(\bar{\boldsymbol{x}}) \leq 0,\ \forall \bar{\boldsymbol{x}} \in \mathbb{R}^3 / \Upsilon_0$ such that the tracking error will converge to a compact set around zero.

Part 2: Following the above analysis that the state of the error system will converge to a compact set around the origin for all the $\boldsymbol{x} \in \mathbb{R}^2$, then there exists $t_c > 0$ such that $\boldsymbol{x}(t_c) \in \partial \bar{C}$ if the initial values of states are not located in the set $\bar{C}$. Thus, once the state enters the set $\bar{C}$ when $t \geq t_c$, the prescribed performance tracking tasks are achieved following the results in **Part 1**. This completes the proof. □

REFERENCES

[1] F. Aghili, J. M. Hollerbach, and M. Buehler, "A modular and high-precision motion control system with an integrated motor," *IEEE/ASME Transactions on Mechatronics*, vol. 12, no. 3, pp. 317–329, 2007.

[2] S.-H. Hyon, "A motor control strategy with virtual musculoskeletal systems for compliant anthropomorphic robots," *IEEE/ASME Transactions on Mechatronics*, vol. 14, no. 6, pp. 677–688, 2009.

[3] A. Bosso, C. Conficoni, D. Raggini, and A. Tilli, "A computational-effective field-oriented control strategy for accurate and efficient electric propulsion of unmanned aerial vehicles," *IEEE/ASME Transactions on Mechatronics*, vol. 26, no. 3, pp. 1501–1511, 2020.

[4] M. Jacquet, M. Kivits, H. Das, and A. Franchi, "Motor-level n-mpc for cooperative active perception with multiple heterogeneous uavs," *IEEE Robotics and Automation Letters*, vol. 7, no. 2, pp. 2063–2070, 2022.

[5] S. K. Kommuri, M. Defoort, H. R. Karimi, and K. C. Veluvolu, "A robust observer-based sensor fault-tolerant control for pmsm in electric vehicles," *IEEE Transactions on Industrial Electronics*, vol. 63, no. 12, pp. 7671–7681, 2016.

[6] X. Liu, H. Chen, J. Zhao, and A. Belahcen, "Research on the performances and parameters of interior pmsm used for electric vehicles," *IEEE Transactions on Industrial Electronics*, vol. 63, no. 6, pp. 3533–3545, 2016.

[7] J.-H. She, M. Fang, Y. Ohyama, H. Hashimoto, and M. Wu, "Improving disturbance-rejection performance based on an equivalent-input-disturbance approach," *IEEE Transactions on Industrial Electronics*, vol. 55, no. 1, pp. 380–389, 2008.

[8] H. Liu and S. Li, "Speed control for pmsm servo system using predictive functional control and extended state observer," *IEEE Transactions on Industrial Electronics*, vol. 59, no. 2, pp. 1171–1183, 2011.

[9] M. Preindl and S. Bolognani, "Model predictive direct speed control with finite control set of pmsm drive systems," *IEEE Transactions on Power Electronics*, vol. 28, no. 2, pp. 1007–1015, 2012.

[10] J. Yao, Z. Jiao, D. Ma, and L. Yan, "High-accuracy tracking control of hydraulic rotary actuators with modeling uncertainties," *IEEE/ASME Transactions on Mechatronics*, vol. 19, no. 2, pp. 633–641, 2013.

[11] Y. Yan, J. Yang, Z. Sun, C. Zhang, S. Li, and H. Yu, "Robust speed regulation for pmsm servo system with multiple sources of disturbances via an augmented disturbance observer," *IEEE/ASME Transactions on Mechatronics*, vol. 23, no. 2, pp. 769–780, 2018.

[12] S. Wang and J. Na, "Parameter estimation and adaptive control for servo mechanisms with friction compensation," *IEEE Transactions on Industrial Informatics*, vol. 16, no. 11, pp. 6816–6825, 2020.

[13] S. Du, B. Cao, and X. Li, "Observer-based distributed model predictive control of complex systems with state coupling constraints," *IET Control Theory & Applications*, vol. 16, no. 13, pp. 1364–1372, 2022.

[14] Y. Zhang and C. Hua, "Composite learning finite-time control of robotic systems with output constraints," *IEEE Transactions on Industrial Electronics*, vol. 70, no. 2, pp. 1687–1695, 2022.

[15] X. Wang, M. Reitz, and E. E. Yaz, "Field oriented sliding mode control of surface-mounted permanent magnet ac motors: Theory and applications to electrified vehicles," *IEEE Transactions on Vehicular Technology*, vol. 67, no. 11, pp. 10 343–10 356, 2018.

[16] Y. Yan, X.-F. Wang, B. J. Marshall, C. Liu, J. Yang, and W.-H. Chen, "Surviving disturbances: A predictive control framework with guaranteed safety," *Automatica*, vol. 158, p. 111238, 2023.

[17] A. Ilchmann, E. P. Ryan, and C. J. Sangwin, "Tracking with prescribed transient behaviour," *ESAIM: Control, Optimisation and Calculus of Variations*, vol. 7, pp. 471–493, 2002.

[18] T. Berger, H. H. Lê, and T. Reis, "Funnel control for nonlinear systems with known strict relative degree," *Automatica*, vol. 87, pp. 345–357, 2018.

[19] C. P. Bechlioulis and G. A. Rovithakis, "Robust adaptive control of feedback linearizable mimo nonlinear systems with prescribed performance," *IEEE Transactions on Automatic Control*, vol. 53, no. 9, pp. 2090–2099, 2008.

[20] C. P. Bechlioulis and G. A. Rovithakis, "A low-complexity global approximation-free control scheme with prescribed performance for unknown pure feedback systems," *Automatica*, vol. 50, no. 4, pp. 1217–1226, 2014.

[21] J. Na, Q. Chen, X. Ren, and Y. Guo, "Adaptive prescribed performance motion control of servo mechanisms with friction compensation," *IEEE Transactions on Industrial Electronics*, vol. 61, no. 1, pp. 486–494, 2013.

[22] S. Wang, X. Ren, J. Na, and T. Zeng, "Extended-state-observer-based funnel control for nonlinear servomechanisms with prescribed tracking performance," *IEEE Transactions on Automation Science and Engineering*, vol. 14, no. 1, pp. 98–108, 2016.

[23] B. Ding, D. Xu, B. Jiang, P. Shi, and W. Yang, "Disturbance-observer-based terminal sliding mode control for linear traction system with prescribed performance," *IEEE Transactions on Transportation Electrification*, vol. 7, no. 2, pp. 649–658, 2020.

[24] Y. Cheng, X. Ren, D. Zheng, and L. Li, "Non-linear bandwidth extended-state-observer based non-smooth funnel control for motor-drive servo systems," *IEEE Transactions on Industrial Electronics*, vol. 69, no. 6, pp. 6215–6224, 2021.

[25] Z. Guo, D. Henry, J. Guo, Z. Wang, J. Cieslak, and J. Chang, "Control for systems with prescribed performance guarantees: An alternative interval theory-based approach," *Automatica*, vol. 146, p. 110642, 2022.
[26] K. Yong, M. Chen, Y. Shi, and Q. Wu, "Flexible performance-based robust control for a class of nonlinear systems with input saturation," *Automatica*, vol. 122, p. 109268, 2020.
[27] T. Berger, "Input-constrained funnel control of nonlinear systems," *IEEE Transactions on Automatic Control*, 2024.
[28] X. Xu, P. Tabuada, J. W. Grizzle, and A. D. Ames, "Robustness of control barrier functions for safety critical control," *IFAC-PapersOnLine*, vol. 48, no. 27, pp. 54–61, 2015.
[29] A. D. Ames, X. Xu, J. W. Grizzle, and P. Tabuada, "Control barrier function based quadratic programs for safety critical systems," *IEEE Transactions on Automatic Control*, vol. 62, no. 8, pp. 3861–3876, 2017.
[30] W. Xiao and C. Belta, "High order control barrier functions," *IEEE Transactions on Automatic Control*, vol. 67, no. 7, pp. 3655–3662, 2022.
[31] W.-H. Chen, J. Yang, L. Guo, and S. Li, "Disturbance-observer-based control and related methods - an overview," *IEEE Transactions on Industrial Electronics*, vol. 63, no. 2, pp. 1083–1095, 2015.
[32] X. Xu, "Constrained control of input–output linearizable systems using control sharing barrier functions," *Automatica*, vol. 87, pp. 195–201, 2018.
[33] M. Johansson and A. Rantzer, "Computation of piecewise quadratic lyapunov functions for hybrid systems," in *1997 European Control Conference (ECC)*, pp. 2005–2010. IEEE, 1997.
[34] W. Xue, R. Madonski, K. Lakomy, Z. Gao, and Y. Huang, "Add-on module of active disturbance rejection for set-point tracking of motion control systems," *IEEE Transactions on Industry Applications*, vol. 53, no. 4, pp. 4028–4040, 2017.
[35] W.-H. Chen, D. J. Ballance, P. J. Gawthrop, and J. O'Reilly, "A nonlinear disturbance observer for robotic manipulators," *IEEE Transactions on Industrial Electronics*, vol. 47, no. 4, pp. 932–938, 2000.
[36] H. K. Kahlil, *Nonlinear systems.* (3rd ed.). Prentice Hall, 2002.
[37] S. Boyd, S. P. Boyd, and L. Vandenberghe, *Convex optimization*. Cambridge University Press, 2004.
[38] Z. Gao *et al.*, "Scaling and bandwidth-parameterization based controller tuning," in *American Control Conference*, pp. 4989–4996, 2003.
[39] Q.-C. Zhong, A. Kuperman, and R. Stobart, "Design of ude-based controllers from their two-degree-of-freedom nature," *International Journal of Robust and Nonlinear Control*, vol. 21, no. 17, pp. 1994–2008, 2011.
[40] J.-H. She, X. Xin, and Y. Pan, "Equivalent-input-disturbance approach-analysis and application to disturbance rejection in dual-stage feed drive control system," *IEEE/ASME Transactions on Mechatronics*, vol. 16, no. 2, pp. 330–340, 2010.
[41] K. Kuttler, *Linear algebra: theory and applications*. The Saylor Foundation, 2012.

Xinming Wang (Graduate Student Member, IEEE) received the B.E. degree and M.E. degree in navigation, guidance and control from Northwestern Polytechnical University, Xi'an, China, in 2016 and 2019, respectively. He is now pursuing a Ph.D. degree from the School of Automation of Southeast University, Nanjing, China. He has been a visiting student with the Department of Aeronautical and Automotive Engineering, Loughborough University, UK, since 2022. His research interests include safety-critical control, disturbance rejection control, and its applications to mechatronics systems and flight control systems.

Yuan Jiang was born in Suqian, China, in 1998. He received his B.E. degree in electrical engineering and automation from Nanjing Institute of Technology, China, in 2019. He is currently working toward a Ph.D. degree in control theory and control engineering from the School of Automation, Southeast University, Nanjing, China. His research interests include motion control, disturbance/uncertainty estimation, and attenuation theory with applications to mechatronic systems.

Jun Yang (Fellow, IEEE) received the B.Sc. degree in automation from the Department of Automatic Control, Northeastern University, Shenyang, China, and the Ph.D. degree in control theory and control engineering from the School of Automation, Southeast University, Nanjing, China, in 2006 and 2011, respectively. Since 2020, he has been with the Department of Aeronautical and Automotive Engineering, Loughborough University, Loughborough, U.K., as a Senior Lecturer and is promoted to a Reader in 2023. His research interests include disturbance observer, motion control, visual servoing, nonlinear control, and autonomous systems. Dr. Yang was the recipient of the EPSRC New Investigator Award.

He serves as an Associate Editor or Technical Editor for IEEE Transactions on Industrial Electronics, IEEE-ASME Transactions on Mechatronics, IEEE Open Journal of Industrial Electronics Society, etc. He is a Fellow of IEEE and IET.

Yunda Yan (Member, IEEE) received the BEng degree in automation and the Ph.D. degree in control theory and control engineering from the School of Automation, Southeast University, Nanjing, China, in 2013 and 2019, respectively. From 2016 to 2018, he was a visiting scholar in the Department of Biomedical Engineering, National University of Singapore, Singapore and the Department of Aeronautical and Automotive Engineering, Loughborough University, UK, respectively. From 2020 to 2022, he was a Research Associate with the Department of Aeronautical and Automotive Engineering, Loughborough University, UK. From 2022 to 2023, he was with the School of Engineering and Sustainable Development, De Montfort University, UK, as a Lecturer in Control Engineering and was later promoted to a Senior Lecturer. In September 2023, he joined the Department of Computer Science, University College London, UK, as a Lecturer in Robotics and AI. His current research interest focuses on the safety-guaranteed control design for robotics, especially related to optimization, data-driven, and learning-based methods.

Shihua Li (Fellow, IEEE) received his B.S., M.S. and Ph.D. degrees in automatic control from Southeast University, Nanjing, China, in 1995, 1998, and 2001, respectively. Since 2001, he has been with the School of Automation, Southeast University, where he is currently a Full Professor and the Director of Mechatronic Systems Control Laboratory. His main research interests lie in modeling, analysis, and nonlinear control theory with applications to mechatronic systems, including robots, AC motors, engine control, power electronic systems, and others.